Parasitology Research (2020) 119:1653–1661
https://doi.org/10.1007/s00436-020-06665-9

PROTOZOOLOGY - ORIGINAL PAPER

Preliminary study of the mechanism of action of ethanamizuril against *Eimeria tenella*

Xueyan Li[1] · Huiya Chen[1] · Qiping Zhao[1] · Lifang Zhang[1] · Keyu Zhang[1] · Xiaoyang Wang[1] · Mi Wang[1] · Yingchun Liu[1] · Chunmei Wang[1] · Feiqun Xue[1] · Chenzhong Fei[1]

Received: 16 May 2019 / Accepted: 15 March 2020 / Published online: 26 March 2020

Abstract

Ethanamizuril (EZL) is a novel triazine compound with excellent anticoccidial activity. We carried out a preliminary investigation of the effects of EZL on the different life cycle stages of *Eimeria tenella*. EZL mainly acted on the schizogony stage, with peak activity during the second-generation merozoite stage. We also studied the possible target of EZL by identifying the majorly differentially expressed gene affected by EZL in second-generation merozoites using real-time polymerase chain reaction, and screening for surface antigen proteins (SAGs). The relative expression levels of SAGs were compared by Western blot analysis showing that expression levels of surface antigen family member (SAGfm) and SAG19 were significantly downregulated by EZL. Immunofluorescence analysis indicated that SAGfm and SAG19 were localized on the surface of second-generation merozoites. In addition, fluorescence signals were significantly stronger in second-generation merozoites of infected non-medicated control (INC) group compared with that of the EZL group. Therefore, it was speculated that SAGs might be a potential target of EZL action. The inhibitory effects of anticoccidial drugs on SAG levels in coccidia thus warrant further research.

Keywords *Eimeria tenella* · Ethanamizuril · Mechanism of action · Surface antigen protein

Introduction

Coccidiosis is an intracellular parasitic disease caused by coccidia, resulting in huge economic losses to the chicken-breeding industry every year (Shirley et al. 2007; Williams 1999). *Eimeria tenella* has been regarded as a highly pathogenic species responsible for cecal coccidiosis. For the limitation of clinical use of vaccines, the prophylaxis and treatment of avian coccidiosis depend mainly on chemical drugs (Blake and Tomley 2014; Dalloul and Lillehoj 2006). However, the long-term use of anticoccidial drugs has inevitably led to the emergence of drug resistance, and there is thus an urgent need to develop new therapeutic drugs and strategies to control coccidiosis (Tan et al. 2017; Witcombe and Smith 2014).

Triazines are widely used anticoccidial drugs, to which resistance has also appeared in recent years (Stock et al. 2018). Ethanamizuril (EZL) is a new triazine compound synthesized by Shanghai Veterinary Research Institute, Chinese Academy of Agricultural Sciences. EZL has shown high anticoccidial activity, low toxicity, and no genotoxicity or teratogenicity (Fei et al. 2013; Zhang et al. 2019); however, its exact mechanism of action remains unknown. Anticoccidial drugs might act by upregulating or downregulating the expression levels of functional proteins in coccidia. Diclazuril affected heat shock protein (Hsp) 90 in second-generation merozoites of *E. tenella*, thus furthering the understanding of the molecular mechanism of chemotherapy and suggesting that Hsp90 might represent a promising target for interventions aimed at *E. tenella* infection (Shen et al. 2012). Lower aspartate aminotransferase and higher lactate dehydrogenase activities in birds with coccidiosis treated with toltrazuril indicated that this treatment aided the regeneration of digestive system tissues (Sokół et al. 2015). Furthermore, previous studies showed that EZL interfered with metabolism by inhibiting the expression of enolase of *E. tenella* (Liu et al. 2016b).

Section Editor: David S. Lindsay

✉ Chenzhong Fei
aries@shvri.ac.cn

[1] Key Laboratory of Veterinary Chemical Drugs and Pharmaceutics, Ministry of Agriculture and Rural Affairs; Shanghai Veterinary Research Institute, Chinese Academy of Agricultural Sciences, No. 518, Ziyue Road, Minhang District 200241, Shanghai, People's Republic of China

Surface antigen proteins (SAGs) are glycosylphosphatidylinositol (GPI)-anchored surface proteins that are differentially regulated among oocysts, sporozoites, and second-generation merozoites of *E. tenella*, including 37 known and many unannotated proteins (Tabarés et al. 2004). SAGs have been shown to activate an immune response in chickens against *E. tenella*. The SAG gene of *Eimeria maxima* (*Em*SAG) could also stimulate immune protection against *E. maxima* (Chow et al. 2011; Liu et al. 2018). Several GPI-anchored antigens on the surface of parasite cell membranes have been considered to be major determinants of critical interactions with host cells. Dzierszinski et al. (2000) reported that SAG3 of *Toxoplasma gondii* could decrease host cell adhesion. However, although the expression of SAGs might be related to the mechanism of action of anticoccidial drugs, the mechanism of drug action on SAGs is not clear yet.

In this study, we investigated the action of EZL in relation to the developmental stage of *E. tenella* by evaluating its efficacy at different stages of the life cycle. Furthermore, we verified differentially expressed SAGs between EZL-treated and untreated *E. tenella* during the peak period of action by real-time polymerase chain reaction (PCR), Western blot, and immunofluorescence localization analysis to explore the potential target of EZL.

Materials and methods

Drugs and parasite

EZL (> 98%) and diclazuril (> 98%) were provided by Shanghai Veterinary Research Institute, Chinese Academy of Agriculture Sciences. The strain of *E. tenella* was isolated and maintained by the Key Laboratory of Animals Parasitology of the Ministry of Agriculture and Rural Affairs. Sporulated oocysts were stored in 2.5% potassium dichromate at 4 °C to maintain their viability and rejuvenated before infection.

Chickens

One-day-old Pudong yellow broiler chicks were purchased from a local hatchery (Shanghai, China) and reared in a coccidia-free environment. The chicks were provided with water and a standard diet without drug supplements ad libitum. Electric radiators and ventilation fans were used to maintain the recommended temperature and 24-h lighting. The experimental protocol was conformed to the guidelines of the Institutional Animal Care and Use Committee of China, and was approved by the Ethics Committee of Shanghai Veterinary Research Institute, Chinese Academy of Agricultural Sciences.

Efficacy evaluation of EZL at different stages of the life cycle of *E. tenella*

Four hundred 12-day-old chickens were weighed and allocated randomly to 10 groups ($n = 40$ per group): A1–A8, infected non-medicated control (INC), and non-infected non-medicated control (NNC). Each group was further subdivided into four blocks as four biological replicates of 10 chickens each. Chickens in groups A1–A8 and INC were infected by oral gavage with 8×10^4 *E. tenella*–sporulated oocysts per chicken. Chickens in groups A1–A7 were given 10 mg/kg EZL in feed for 3 consecutive days at different stages, and group A8 was administered continuous 1 mg/kg diclazuril in feed, whereas groups INC and NNC were provided with standard diet without drug supplements (Table 1). All chickens were sacrificed on the eighth day after infection.

Anticoccidial activity was assessed by measuring survival rate (SR), weight gain (WG), oocyst index (OI), oocyst production of per gram feces (OPG), and lesion gain (LS) according to the guidelines for evaluating the efficacy of anticoccidial drugs in chickens (Holdsworth et al. 2004). The overall efficacy was mainly evaluated by anticoccidial index (ACI), with ACI > 180 considered excellent activity, 160–179 moderate activity, 120–159 limited activity, and < 120 inefficacy (Suo and Li 1998).

Extraction and purification of second-generation merozoites of *E. tenella*

A total of 120 chickens at approximately 2 weeks old were allocated randomly to the INC group and EZL group ($n = 60$ per group). Each group was further subdivided into three blocks as three biological replicates of 20 chickens each. Then, all the chickens were orally infected with 8×10^4 *E. tenella*–sporulated oocysts per chicken. Chickens in the EZL group were given 10 mg/kg EZL at 96 h post infection, while chickens in the INC group did not receive any treatment. Chickens were sacrificed at 116 h post infection, and cecal tissues were collected and processed for the extraction and purification of second-generation merozoites of *E. tenella*, as described previously (Shen et al. 2014).

mRNA levels of differentially expressed proteins in second-generation merozoites of *E. tenella* determined by real-time PCR

Total RNA was extracted from second-generation merozoites using an RNeasy®Mini Kit (Qiagen, Germany). The quantity and quality of the extracted RNA were measured by gel electrophoresis and an Ulrtramicro spectrophotometer (Thermo Fisher, USA). First-strand cDNA was synthesized from 2 μg total RNA according to the GoScript™ Reverse Transcription System protocol (Qiagen, Germany).

Table 1 Efficacy evaluation of EZL at different stages of life cycle of *E. tenella*

Group	Administration time (day)	SR (%)	WG	OPG	OI	LS	ACI
A1	− 2~1	95	223 ± 51	46.9 ± 10.5	40	24	104 ± 11
A2	− 1~2	85	214 ± 54	80.7 ± 17.0	40	23	92 ± 11
A3	0~3	100	257 ± 44	23.2 ± 13.2	40	19	125 ± 16**
A4	1~4	100	297 ± 35	9.2 ± 4.8	10	17	170 ± 8**
A5	2~5	100	296 ± 33	0.4 ± 0.5	5	1	191 ± 5**
A6	3~6	100	272 ± 37	0.2 ± 0.2	0	18	171 ± 4**
A7	4~7	98	248 ± 54	0.3 ± 0.3	0	18	161 ± 5**
A8	0~7	100	295 ± 33	0.0	0	15	181 ± 14**
INC	--	78	194 ± 55	27.4 ± 8.0	40	27	73 ± 31**
NNC	--	100	306 ± 22	0.0	0	0	200 ± 2

SR, survival rate; *WG*, weight gain; *OPG*, oocyst production of per gram feces; *LS*, lesion gain; *OI*, oocyst index; *ACI*, anticoccidial index; *Administration time*, the day of infection as day 0; *A1–A7*: EZL, 10 mg/kg; *A8*: diclazuril, 1 mg/kg; *INC*, infected non-medicated control; *NNC*, non-infected non-medicated control

**Means with the same letters were significant difference ($P < 0.05$)

Reverse transcription products from second-generation merozoites were amplified by real-time PCR to verify the mRNA levels of differentially expressed proteins. Real-time PCR was performed in an optical 96-well plate with an ABI-7500 real-time PCR System (Applied Biosystems, USA) using specific primers (Table 2) and cycling conditions (I, 2 min at 95 °C; II, 40 cycles of 15 s at 95 °C, 1 min at 60 °C; III, dissociation stage). The reaction mixture contained 10 μl GoTaq® qPCR Master Mix (Promega, USA), 0.4 μl forward primer (200 nM), 0.4 μl reverse primer (200 nM), 2 μl cDNA (≥ 100 ng), and 7.2 μl nuclease-free water in each 20 μl reaction mixture. The housekeeping gene β-actin was used as an endogenous control to normalize the relative expression levels of differential proteins between groups. Quantitative analysis was carried out using the comparative CT method (Schmittgen 2001). Negative controls were needed to be established for each trial. Each reaction was performed in triplicate, and each experiment was carried out twice.

Generation of recombinant SAGs

Recombinant SAGs (rSAGs) was constructed as previously described (Mai et al. 2007). Briefly, the open reading frames (ORFs) of SAGfm and SAG19 without the signal peptide sequences were amplified using specific primers (Table 3) for PCR assays with *E. tenella* cDNA as a template, respectively. The amplification products of SAGfm and SAG19 were then cloned using a pGEM-T Easy vector (TaKaRa, China), inserted into the expression vector pET-28a (+) (Novagen, China), and confirmed by endonuclease digestion. Following sequence analysis (Sangon Biotech, Shanghai, China) and verification, the positive clones were confirmed as pET-28a-SAGfm and pET-28a-SAG19 and induced to abundantly express at different temperatures and isopropyl β-d-1-thiogalactopyranoside concentrations in *Escherichia coli* BL21 (DE3). Then, rSAGs were purified using His GraviTrap (GE, USA) and the concentration of the samples was determined using the Bradford method (Ku et al. 2013). The purified rSAGs were verified by sodium dodecyl sulfate-polyacrylamide gel electrophoresis (SDS-PAGE) and Western blot, and stored at − 80 °C until further analysis.

Preparation of polyclonal anti-SAG antibodies

Rabbit polyclonal anti-SAGfm and anti-SAG19 antibodies were generated in 5-week-old pathogen-free New Zealand white rabbits. Rabbits were immunized subcutaneously with 0.5 mg recombinant proteins fully emulsified with Freund's complete adjuvant. Two weeks after the first immunization, the rabbits were injected with 0.3 mg recombinant protein in Freund's incomplete adjuvant. Three booster immunizations were administered at 1-week intervals. Finally, rabbit serum containing antibodies was harvested after the last booster injection and stored at − 80 °C until subsequent analysis. Pre-immunization serum was obtained for later use as a negative control.

Protein expression levels of SAGs in second-generation merozoites of *E. tenella* determined by Western blot

Total proteins were extracted from second-generation merozoites in the EZL and INC groups using cell lysis buffer (Western and immunoprecipitation buffer, 1% SDS, 1 mM phenylmethylsulfonyl fluoride). Following repeated pipetting to crack the merozoites, lysis buffer was added and centrifuged at 14,000×*g* for 5 min, and the supernatant was then transferred to a new 1.5-ml centrifuge tube. Protein concentrations were quantified using a BCA Protein Assay Kit

Table 2 Specific primer sequences used in real-time PCR analysis

Protein name	Uniprot accession	Primer name	Specific primer sequence(5′–3′)
β-Actin	H9BA70	Forward	GGATTGCTATGTCGGCGATGA
		Reverse	ACACGCAACTCGTTGTAGAAAGTG
Lactate dehydrogenase	Q87804	Forward	CGCCACCTAAGGACGATA
		Reverse	TGCCAAGGGAGCCAAGCA
Phosphoglycerate kinase	U6L816	Forward	CGTCTGGTCAGCAAACCCTA
		Reverse	GACATCCCGCAGTGAGCAAT
Eukaryotic initiation factor 4a	U6KZN0	Forward	TTCAAGGCGCAGATTTTGGC
		Reverse	GACGAGGGTGTCGAACTTGT
Ribosomal protein	U6KW42	Forward	GGCCTCCCCAATTTAGGCTT
		Reverse	CCCAACAAACACGCAAGGAG
Hexokinase	U6KUE1	Forward	TTTCCGGGTTCTACTTGGGC
		Reverse	CAAGTCCCATCCCCAGCTTT
Glyceraldehyde 3-phosphate dehydrogenase	E3VWM6	Forward	CAACGCATCTTGCACAACCA
		Reverse	AGGGGATAACTTTGCCCACG
Superoxide dismutase	U6KTI3	Forward	ACGCCTTTCAGAGACAACCC
		Reverse	TCTCATTCGCGAAGTCCCAA
SAGfm 1	H9B9H4	Forward	GGCCTTAGGGGACAGTTCAC
		Reverse	ATTAAGGCCTTCCGTTCGCA
SAGfm 2	U6KUL4	Forward	CAGACTGCCGAGTTGTCACT
		Reverse	CTGCTATCGATGCGGAACCT
SAGfm 3	Q70CC8	Forward	AAAGCGAATGCGGGGAAGTA
		Reverse	TTTGTGCTTTTCGCCGACAG
SAGfm 4	Q70CD0	Forward	CCCTACTGCGCCGAAAATTG
		Reverse	AGTCCAGCAGTGTAAGTCGC
SAGfm 5	U6L233	Forward	CACGGAGTTCAACTGCAACG
		Reverse	CTCCGATAGCAGAAACGCCA
Eukaryotic initiation factor 4e	U6L048	Forward	AGAAGGCATCCAGCCAATGT
		Reverse	CAGTGACGTGACTTCCGTGT
Ribosomal protein	H9B912	Forward	CAGTGCCCACAAGTTCCCTC
		Reverse	GTCCGTGATGTTGTGACCCT

SAGfm, surface antigen family member

(Beyotime, China) and adjusted to be consistent using phosphate-buffered saline (PBS). Protein samples (20 μg per lane) were detected using 10% SDS-PAGE, and the separated proteins were transferred onto a polyvinylidene difluoride membrane. Subsequently, the membrane was blocked with 5% skimmed milk powder for 2 h, followed by overnight incubation with primary rabbit polyclonal antibodies (1:500 dilution) at 4 °C. After washing in TBST buffer, the

Table 3 Primer sequences used in PCR amplification

Protein name	GeneBank accession	Primer name	Primer sequence(5′–3′)	Restriction enzyme
SAGfm	XM_013378554	Forward	TATGGATCCCTTTCCCTTCGCTCTAGC	BamH I
		Reverse	GCGAAGCTTTCAAGCCCGAATGATCAGAG	Hind III
SAG19	XM_013379462	Forward	TATGGATCCCTACACTTCTCATCGGCG	BamH I
		Reverse	GCGAAGCTTTCAAGCCCGAATGATCAG	Hind III

SAGfm, surface antigen family member. Restriction enzyme sites underlined

membrane was incubated with horse radish peroxidase (HRP)–conjugated goat anti-rabbit IgG (1:1000 dilution, Beyotime, China) for 1 h. Then, after washing in TBST buffer, HRP signals were detected using an enhanced chemiluminescent solution Beyo ECL (Beyotime, China). The expression levels of SAGs were analyzed and quantified using ImageJ 1.46 software to calculate their grayscale values.

Localization of SAGs in second-generation merozoites of *E. tenella*

Second-generation merozoites in the EZL and INC groups were fixed on glass slides using 2% paraformaldehyde for 15–30 min, washed three times with PBS, and then blocked with 2% bovine serum albumin for 2 h. After washing in PBS, the merozoites were incubated overnight with polyclonal antibodies (1:500 dilutions) at 4 °C. The merozoites were then washed in PBS and incubated with fluorescein isothiocyanate (FITC)–conjugated goat anti-rabbit IgG (1:1000 dilution; Beyotime). Nucleus were probed with 2-(4-amidinophenyl)-6-indole carbamidinedihydrochloride (DAPI; Sigma-Aldrich). The glass slides were examined under an inverted fluorescence microscope (Zeiss, Germany).

Statistical analysis

Data were presented as mean ± standard deviation. Results were compared between groups by analysis of variance followed by Bonferroni's *t* test. Differences were considered significant at $p < 0.05$.

Results

Efficacy of EZL at different stages of the life cycle of *E. tenella*

The various parameters used to evaluate efficacy of EZL at different stages of the life cycle of *E. tenella* were summarized in Table 1. These parameters showed that the experiment conformed to the requirements of clinical trials of anticoccidial drugs. The ACIs in groups A8, INC, and NNC were 181 ± 14, 73 ± 31, and 200 ± 2, respectively. The ACIs in groups A1, A2, and A3 were 104 ± 11, 92 ± 11, and 125 ± 16, showing no anticoccidial activities, respectively; the ACIs in groups A4, A6, and A7 were 170 ± 8, 171 ± 4, and 161 ± 5, showing moderate anticoccidial activity, respectively; and the ACI in group A5 was 191 ± 5, indicating excellent anticoccidial activity, corresponding to the developmental stages of second-generation merozoites.

mRNA levels of differentially expressed proteins in second-generation merozoites of *E. tenella* determined by real-time PCR

Seven upregulated and seven downregulated proteins screened by proteomics in second-generation *E. tenella* merozoites under EZL treatment were selected for real-time PCR verification (Table 4). The result of real-time PCR was similar with that of proteomic analysis.

Amplification of SAGs

Full-length SAGs were amplified by PCR with *E. tenella* cDNA as a template. Sequence analysis showed that SAGfm ORF contained 738 bp encoding 246 amino acid residues and SAG19 ORF contained 756 bp encoding 252 amino acid residues (Fig. 1).

Expression and purification of rSAGs

rSAGs were abundantly expressed in the precipitate and were inclusion body proteins, as shown by SDS-PAGE. The purified fusion rSAGfm and rSAG19 were approximately 32.10 kDa and 32.26 kDa, respectively (Fig. 2). This calculated total value of fusion protein was considered the sum of both the approximate 3.52 kDa length of the vector after restriction enzyme digestion and the length of the SAG (SAGfm, 28.58 kDa; SAG19, 28.74 kDa). rSAGfm and rSAG19 verified by Western blot analysis both contained His tags (Fig. 3).

Protein expression levels of SAGs in second-generation merozoites of *E. tenella* determined by Western blot analysis

The protein expression levels of SAGs were analyzed and quantified using the ImageJ 1.46 software to calculate the grayscale values. The expression levels SAGfm and SAG19 were significantly reduced in the EZL group compared with those in the INC group (Figs. 4, 5, and 6), indicating that SAGfm and SAG19 protein expression were significantly downregulated by EZL treatment.

Localization of SAGs in second-generation merozoites of *E. tenella*

We determined the distribution of SAGs in second-generation merozoites of *E. tenella* in the EZL and INC groups by immunofluorescence analysis using anti-SAGfm and anti-SAG19 primary rabbit polyclonal antibodies, respectively, and FITC-conjugated goat anti-rabbit IgG second antibody (Fig. 7). The second-generation merozoites of *E. tenella* in the INC group showed good morphology and strong green

Table 4 mRNA levels of differentially expressed proteins in second-generation merozoites of *E. tenella* determined by real-time PCR

Upregulated protein	Uniprot accession	Ratio Log2(S/D)	$2^{-\Delta\Delta CT}$	Downregulated protein	Uniprot accession	Ratio Log2(S/D)	$2^{-\Delta\Delta CT}$
Lactate dehydrogenase	Q8I8U4	1.99	1.74	SAGfm1	H9B9H4	− 1.32	0.0002
Phosphoglycerate kinase	U6L816	1.82	3.26	SAGfm2	U6KUL4	− 1.46	0.015
Eukaryotic transcription initiation factor 4a	U6KZN0	1.46	8.88	SAGfm3	Q70CC8	− 1.46	0.23
Ribosomal protein	U6KW42	1.24	10.54	SAGfm4	Q7OCDO	− 2.47	0.17
Hexokinase	U6KUE1	1.21	200	SAGfm5	U6L233	− 2.76	0.24
Glyceraldehyde 3-phosphate dehydrogenase	E3VWM6	1.16	60	Eukaryotic transcription initiation factor 4e	U6L0A8	− 1.49	0.04
Superoxide dismutase	U6KTI3	1.4	208	60S acidic ribosomal protein P1	H9B912	− 1.5	0.12

SAG fm, surface antigen family member; *Ratio Log2(S/D)*, ratio of protein abundance in EZL group (S) to that in INC group (D) by proteomic analysis

fluorescence signals distributed across the whole surface of the merozoites, indicating that SAGfm and SAG19 were distributed uniformly on the surface of the merozoites. However, the green fluorescence signals were significantly weaker in the EZL group and the outer membrane of the merozoites appeared convex and invaginated. These results showed that the expression levels of SAGs were significantly decreased, and the morphology of merozoites was damaged by EZL treatment.

Discussion

To gain a better understanding of the mechanism of action of anticoccidial drugs, it is necessary to clarify the developmental stages at which they are active. In this study, we evaluated the efficacies of EZL against the different stages of life cycle of *E. tenella*. EZL administration starting 2, 1, and 0 days before infection (groups A1, A2, A3) and lasting for 3 days failed to control the infection, suggesting that EZL had little inhibitory effect on the initial invasive stages of *E. tenella*. However, EZL administration on the first day after infection inhibited the invasion of *E. tenella*, corresponding to the early schizogony stage. EZL also exhibited high anticoccidial activity in the second-generation merozoite and early gametogenesis stages. These results indicated that EZL acted mainly on the schizogony stage, with peak activity against second-generation merozoites. Second-generation merozoites represent an important stage in the coccidian life cycle; during this stage, merozoites reproduce exponentially, resulting in irreversible damage to the intestinal tract in chickens. Diclazuril was also reported to induce apoptosis and alter the mitochondrial transmembrane potential in second-generation merozoites of *E. tenella* (Zhou et al. 2010). We therefore used second-generation merozoites to study the mechanism of EZL action in subsequent experiments.

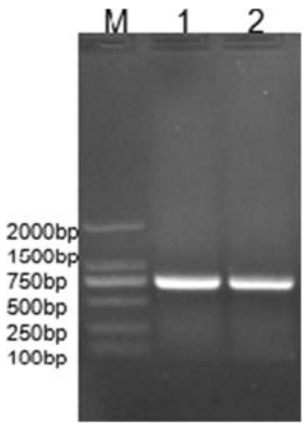

Fig. 1 Amplification of SAGfm and SAG19 genes (cDNA as a template). (M) DNA marker DL2000. (1) PCR product of SAGfm gene. (2) PCR product of SAG19 gene

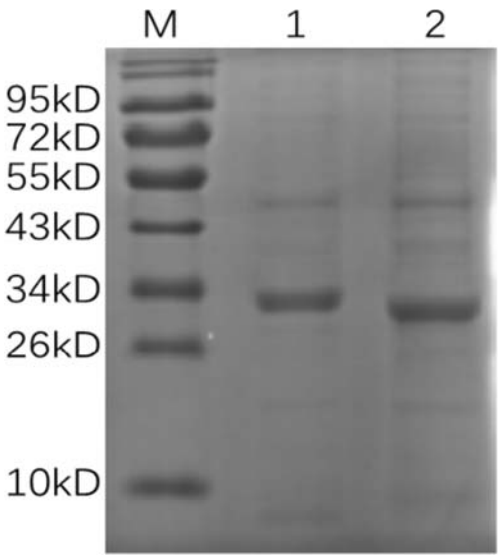

Fig. 2 SDS-PAGE analysis of purified rSAGs. (M) Protein molecular weight marker. (1) Purified rSAGfm. (2) Purified rSAG19.

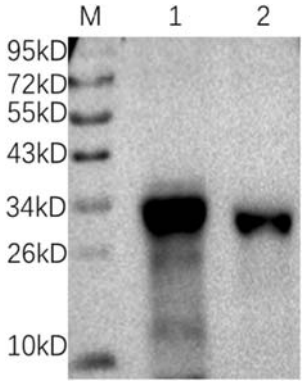

Fig. 3 Western blot analysis of purified rSAGs (6× His monoclonal antibody as primary antibody). (M) Protein molecular weight marker. (1) Purified rSAGfm. (2) Purified rSAG19

Previous studies confirmed that anticoccidial drugs might exhibit their effects by upregulating or downregulating coccidial proteins. Diclazuril reduced the expression of Hsp90, protein kinase C receptor, lactate dehydrogenase, and other proteins (Shen et al. 2012; Shen et al. 2014). Similar to diclazuril, EZL could also downregulate the expression of enolase in second-generation merozoites of *E. tenella*, thus elucidating that EZL exerted anticoccidial activity by interfering with merozoite metabolism (Liu et al. 2016b). After EZL treatment, seven upregulated and seven downregulated proteins were selected from among the differentially expressed coccidial proteins for verification by real-time PCR, which showed that SAGs were significantly downregulated and accounted for a large proportion of the differentially expressed proteins. The levels of *E. tenella* SAGs were regulated differently among oocysts, sporozoites, and second-generation merozoite stages, with only one expressed specifically in sporozoites, a few in both sporozoites and merozoites, and most in second-generation merozoites (Tabarés et al. 2004). Immunoproteomic analysis can also be used to identify differentially expressed proteins in second-generation merozoites, and significant differences in SAGs have been observed (Liu et al. 2009). Overall, these results suggested that SAGs might be involved in the anticoccidial mechanism of EZL.

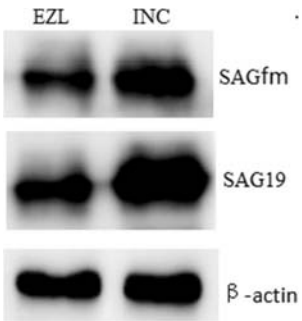

Fig. 4 Western blot analysis of SAGs in the second-generation merozoites of *E. tenella.* EZL: SAGs in the EZL group. INC: SAGs in the INC group

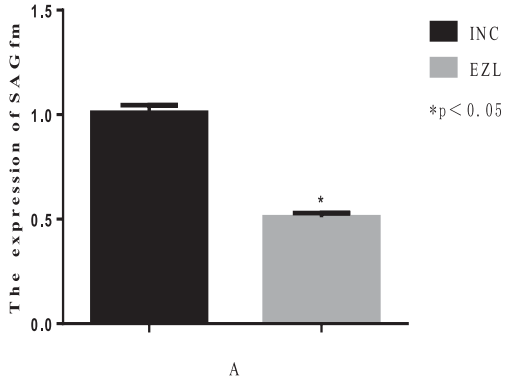

Fig. 5 The protein expression level of SAGfm in the second-generation merozoites of *E. tenella*. EZL: SAGfm in the EZL group. INC: SAGfm in the INC group. *$p < 0.05$ with the same letter was significant difference

In this experiment, SAGfm and SAG19 were significantly downregulated and were validated by molecular methods. Protein levels of SAGfm and SAG19 were significantly lower in the EZL group compared with those in the INC group, in accord with the results of real-time PCR. SAG19, as a representative member of the SAG family, was overexpressed in *Escherichia coli*, purified, and crystallized by the hanging-drop method of vapor diffusion using ammonium sulfate as precipitant (Ramly et al. 2013). The structure of SAG19 has thus been determined, making it suitable for studying the biological function of the drug–protein junction. Many other, unannotated SAGs, such as SAGfm, also have functions similar to SAG19.

We carried out immunofluorescence localization analysis in second-generation merozoites of *E. tenella*, which were non-adherent cells, allowing the entire procedure to be performed in a 1.5-ml centrifuge tube. The fixative and washing solution were removed by centrifugation to avoid damage to and loss of merozoites during the washing process because of their non-adherent nature. In addition, SAGfm and SAG19 were shown to be distributed throughout the surface of the merozoites, but the green fluorescent signal was significantly

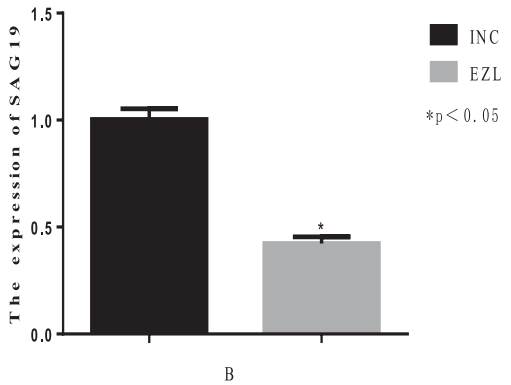

Fig. 6 The protein expression level of SAG19 in the second-generation merozoites of *E. tenella.* EZL: SAG19 in the EZL group. INC: SAG19 in the INC group. *$p < 0.05$ with the same letter was significant difference

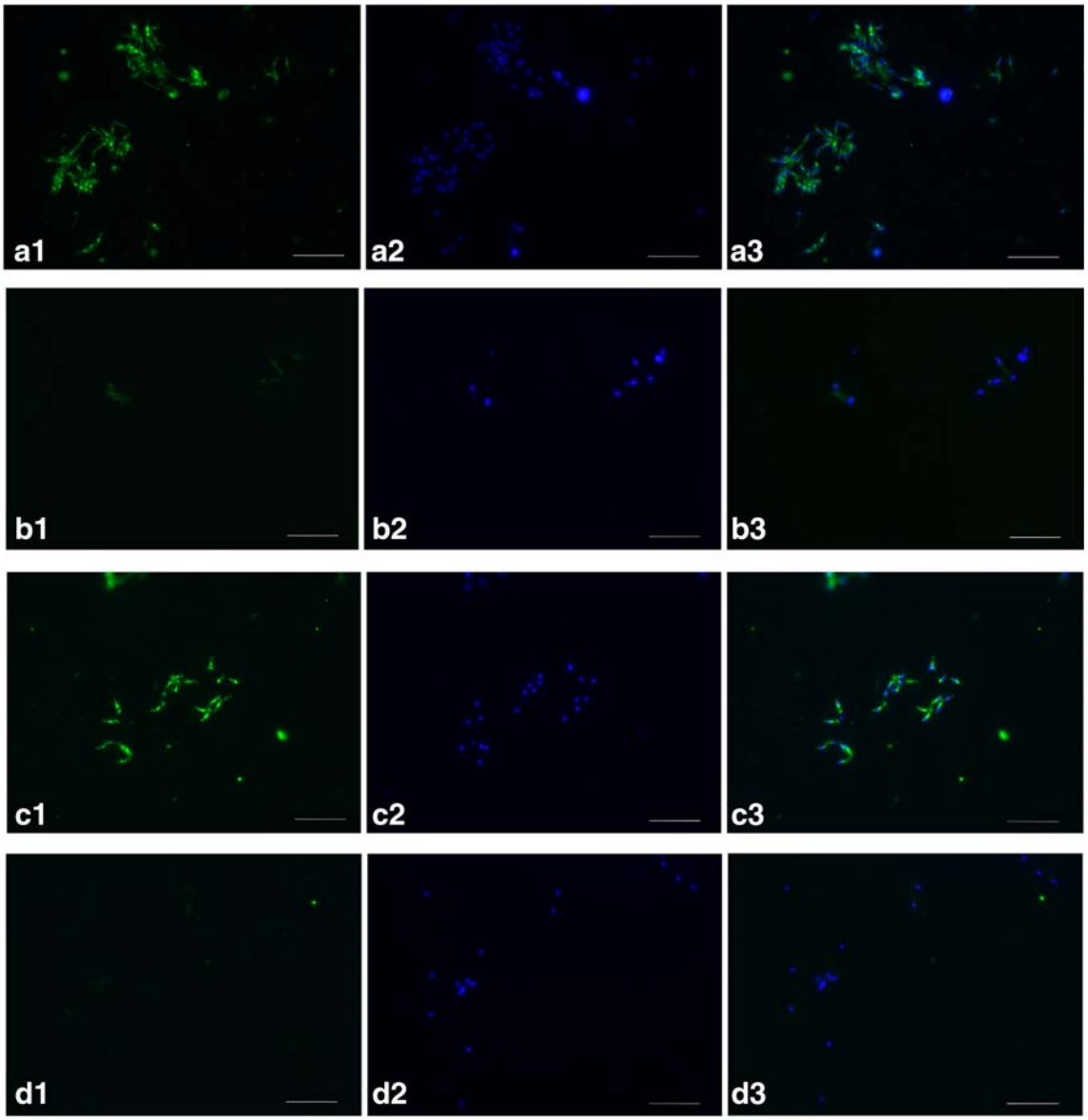

Fig. 7 Location of SAGs in the second-generation merozoites of *E. tenella* at × 40 magnification. A/B: SAGfm in the second-generation merozoites were detected by rabbit polyclonal antibody anti-SAGfm. A1-A3: infected non-medicated control; B1-B3: EZL group. C/D: SAG19 in the second-generation merozoites were detected by rabbit polyclonal antibody anti-SAG19. C1-C3: infected non-medicated control; D1-D3: EZL group. A1, B1, C1, D1: The second-generation merozoites were dyed by FITC. A2, B2, C2, D2: The nuclei were probed by DAPI. A3, B3, C3, D3: Overlaps of FITC and DAPI. Scale-bars 10 μm (Green, Alexa Fluor488-conjugated secondary antibody. Blue, the nuclear dye with DAPI)

weakened in the EZL group and the outer membrane appeared convex and invaginated. These results indicated that EZL significantly inhibited the expression of SAGs and suggested that EZL might destroy the structure of the merozoites by affecting the normal synthesis of SAGs, consistent with the observed damage and ultrastructural changes caused by EZL (Liu et al. 2016a). It was speculated that SAGs might be the target proteins of EZL, and further studies on the mechanism of EZL action are warranted to provide guidance for the development of other anticoccidial drugs to help delay the occurrence of drug resistance.

Conclusion

EZL mainly acted at the schizogony stage of *E. tenella*, with peak activity in second-generation merozoites. Fourteen differentially expressed proteins in second-generation merozoites following EZL treatment were verified by real-time PCR, and SAGs were identified as potential targets of EZL. SAGfm and SAG19 were cloned, expressed, and evaluated by Western blot and immunofluorescence localization, which showed that their expression levels were significantly decreased by EZL. SAGs may thus represent the target proteins

of EZL in *E. tenella*, and further studies are needed to clarify the effects of EZL on coccidial SAGs expression.

Funding information This study was supported by the National Key Research and Development Program of China (2016YFD0501303) and the National Natural Science Foundation of China (31672610).

Compliance with ethical standards

The experimental protocol was conformed to the guidelines of the Institutional Animal Care and Use Committee of China, and was approved by the Ethics Committee of Shanghai Veterinary Research Institute, Chinese Academy of Agricultural Sciences.

Conflict of interest The authors declare that they have no competing interests.

References

Blake DP, Tomley FM (2014) Securing poultry production from the ever-present Eimeria challenge. Trends Parasitol 30(1):12–19. https://doi.org/10.1016/j.pt.2013.10.003

Chow YP, Wan KL, Blake DP, Tomley F, Nathan S (2011) Immunogenic Eimeria tenella glycosylphosphatidylinositol-anchored surface antigens (SAGs) induce inflammatory responses in avian macrophages. PLoS One 6(9):e25233. https://doi.org/10.1371/journal.pone.0025233

Dalloul RA, Lillehoj HS (2006) Poultry coccidiosis: recent advancements in control measures and vaccine development. Expert Rev Vaccines 5(1):143–163. https://doi.org/10.1586/14760584.5.1.143

Dzierszinski F, Mortuaire M, Cesbron-Delauw MF, Tomavo S (2000) Targeted disruption of the glycosylphosphatidylinositol-anchored surface antigen SAG3 gene in Toxoplasma gondii decreases host cell adhesion and drastically reduces virulence in mice. Mol Microbiol 37(3):574–582. https://doi.org/10.1046/j.1365-2958.2000.02014.x

Fei C, Fan C, Zhao Q, Lin Y, Wang X, Zheng W, Wang M, Zhang K, Zhang L, Li T, Xue F (2013) Anticoccidial effects of a novel triazine nitromezuril in broiler chickens. Vet Parasitol 198(1–2):39–44. https://doi.org/10.1016/j.vetpar.2013.08.024

Holdsworth PA, Conway DP, McKenzie M, Dayton AD, Chapman HD, Mathis GF, Skinner JT, Mundt HC, Williams RB, World Association for the Advancement of Veterinary Parasitology (2004) World Association for the Advancement of Veterinary Parasitology (WAAVP) guidelines for evaluating the efficacy of anticoccidial drugs in chickens and turkeys. Vet Parasitol 121(3–4):189–212. https://doi.org/10.1016/j.vetpar.2004.03.006

Ku HK, Lim HM, Oh KH, Yang HJ, Jeong JS, Kim SK (2013) Interpretation of protein quantitation using the Bradford assay: comparison with two calculation models. Anal Biochem 434(1):178–180. https://doi.org/10.1016/j.ab.2012.10.045

Liu L, Xu L, Yan F, Yan R, Song X, Li X (2009) Immunoproteomic analysis of the second-generation merozoite proteins of Eimeria tenella. Vet Parasitol 164(2–4):173–182. https://doi.org/10.1016/j.vetpar.2009.05.016

Liu L, Chen H, Fei C, Wang X, Zheng W, Wang M, Zhang K, Zhang L, Li T, Xue F (2016a) Ultrastructural effects of acetamizuril on endogenous phases of Eimeria tenella. Parasitol Res 115(3):1245–1252. https://doi.org/10.1007/s00436-015-4861-9

Liu LL, Chen ZG, Mi RS, Zhang KY, Liu YC, Jiang W, Fei CZ, Xue FQ, Li T (2016b) Effect of acetamizuril on enolase in second-generation merozoites of Eimeria tenella. Vet Parasitol 215:88–91. https://doi.org/10.1016/j.vetpar.2015.11.011

Liu T, Huang J, Li Y, Ehsan M, Wang S, Zhou Z, Song X, Yan R, Xu L, Li X (2018) Molecular characterisation and the protective immunity evaluation of Eimeria maxima surface antigen gene. Parasit Vectors 11(1):325. https://doi.org/10.1186/s13071-018-2906-5

Mai B et al (2007) Cloning and prokaryotic expression of the SAG10 gene encoding surface antigen 10 of Eimeria tenella Yangling strain. Vet Sci China 37(9):751–755 (in Chinese)

Ramly NZ, Rouzheinikov SN, Sedelnikova SE, Baker PJ, Chow YP, Wan KL, Nathan S, Rice DW (2013) Crystallization and preliminary crystallographic analysis of a surface antigen glycoprotein, SAG19, from Eimeria tenella. Acta Crystallogr Sect F Struct Biol Cryst Commun 69(Pt 12):1380–1383. https://doi.org/10.1107/S1744309113029734

Schmittgen TD (2001) Real-time quantitative PCR. Methods 25(4):383–385

Shen X et al (2012) Effect of the diclazuril on Hsp90 in the second-generation merozoites of Eimeria tenella. Vet Parasitol 185(2):290–295. https://doi.org/10.1016/j.vetpar.2011.10.018

Shen XJ, Li T, Fu JJ, Zhang KY, Wang XY, Liu YC, Zhang HJ, Fan C, Fei CZ, Xue FQ (2014) Proteomic analysis of the effect of diclazuril on second-generation merozoites of Eimeria tenella. Parasitol Res 113(3):903–909. https://doi.org/10.1007/s00436-013-3721-8

Shirley MW, Smith AL, Blake DP (2007) Challenges in the successful control of the avian coccidia. Vaccine 25(30):5540–5547. https://doi.org/10.1016/j.vaccine.2006.12.030

Sokół R, Gesek M, Raś-Noryńska M, Michalczyk M, Koziatek S (2015) Biochemical parameters in Japanese quails Coturnix coturnix japonica infected with coccidia and treated with Toltrazuril. Pol J Vet Sci 18(1):79–82. https://doi.org/10.1515/pjvs-2015-0010

Stock ML, Elazab ST, Hsu WH (2018) Review of triazine antiprotozoal drugs used in veterinary medicine. J Vet Pharmacol Ther 41(2):184–194. https://doi.org/10.1111/jvp.12450

Suo X, Li GQ (1998) Coccidia and coccidiosis of domestic fowl. China Agricultural University Press, Beijing (in Chinese)

Tabarés E, Ferguson D, Clark J, Soon P-E, Wan K-L, Tomley F (2004) Eimeria tenella sporozoites and merozoites differentially express glycosylphosphatidylinositol-anchored variant surface proteins. Mol Biochem Parasitol 135(1):123–132. https://doi.org/10.1016/j.molbiopara.2004.01.013

Tan L, Li Y, Yang X, Ke Q, Lei W, Mughal MN, Fang R, Zhou Y, Shen B, Zhao J (2017) Genetic diversity and drug sensitivity studies on Eimeria tenella field isolates from Hubei Province of China. Parasit Vectors 10(1):137. https://doi.org/10.1186/s13071-017-2067-y

Williams RB (1999) A compartmentalised model for the estimation of the cost of coccidiosis to the world's chicken production industry. Int J Parasitol 29(8):1209–1229. https://doi.org/10.1016/S0020-7519(99)00086-7

Witcombe DM, Smith NC (2014) Strategies for anti-coccidial prophylaxis. Parasitology 141(11):1379–1389. https://doi.org/10.1017/S0031182014000195

Zhang M, Li X, Zhao Q, She R, Xia S, Zhang K, Zhang L, Wang X, Wang M, Liu Y, Wang C, Zhang J, Xue F, Fei C (2019) Anticoccidial activity of novel triazine compounds in broiler chickens. Vet Parasitol 267:4–8. https://doi.org/10.1016/j.vetpar.2019.01.006

Zhou B, Wang H, Xue F, Wang X, Fei C, Wang M, Zhang T, Yao X, He P (2010) Effects of diclazuril on apoptosis and mitochondrial transmembrane potential in second-generation merozoites of Eimeria tenella. Vet Parasitol 168(3–4):217–222. https://doi.org/10.1016/j.vetpar.2009.11.007